Crystallization-Driven Solution Self-Assembly of Block Copolymers with a Photocleavable Junction

7 AUTHORS, INCLUDING:

Yang Gao
Beihang University(BUAA)
8 PUBLICATIONS   **57** CITATIONS

Huibin Qiu
ShanghaiTech University
28 PUBLICATIONS   **597** CITATIONS

Hang Zhou
University of Toronto
6 PUBLICATIONS   **63** CITATIONS

Robert Harniman
University of Bristol
28 PUBLICATIONS   **155** CITATIONS

Crystallization-Driven Solution Self-Assembly of Block Copolymers with a Photocleavable Junction

Yang Gao,[†] Huibin Qiu,[†] Hang Zhou,[‡] Xiaoyu Li,[†] Robert Harniman,[†] Mitchell A. Winnik,*[,‡] and Ian Manners*[,†]

[†]School of Chemistry, University of Bristol, Bristol BS8 1TS, United Kingdom
[‡]Department of Chemistry, University of Toronto, Toronto, Ontario M5S 3H6, Canada

Ⓢ *Supporting Information*

ABSTRACT: Light-responsive block copolymers have been prepared with a crystallizable core-forming poly-(ferrocenyldimethylsilane) (PFS) block, a corona-forming segment of poly(2-vinylpyridine) (P2VP), and a photo-cleavable *o*-nitrobenzyl (ONB) junction. These PFS-ONB-P2VP materials form monodisperse cylindrical micelles by living crystallization-driven self-assembly in a selective solvent for P2VP. The P2VP coronas were readily removed by photocleavage at the ONB linker, leading to PFS cylinders with a residual percentage of corona chains dependent on the photoirradiation time. Addition of PFS block copolymer unimers to a solution of the cylinders with ca. 10% residual coronal chains led to the formation of branched rather than linear micelles. The synthetic utility of the PFS-ONB-P2VP materials was further demonstrated by the preparation of nearly monodisperse P2VP nanotubes of tunable length using a strategy that also involved corona cross-linking.

The solution self-assembly of block copolymers has attracted widespread interest as a result of the potential of this approach to generate functional nanostructures with different morphologies.[1] Many intriguing self-assembled nano-materials have been prepared recently, including patchy micelles,[2] helices,[3] and toroids.[4] When a stimulus-responsive block is incorporated into the block copolymer,[5] reversible or irreversible morphological transitions can be triggered.[6] Light, in particular, is a highly desirable stimulus, which can be applied remotely in a controlled manner. In response to light exposure, micelles can undergo dissociation, controlled release of small molecules, cross-linking, or morphological transitions.[6c,7] Although a series of very interesting results have been obtained with light-responsive micelles,[8] systems involving block copolymers with a photocleavable group at the block junction are much less explored.[8e,9]

We have previously shown that block copolymers with a crystallizable poly(ferrocenyldimethylsilane) (PFS) core-form-ing block can self-assemble into cylindrical micelles in selective solvents for the corona-forming block. Significantly, the termini of the crystalline PFS micelle core remain active for further growth via a process termed living crystallization-driven self-assembly (CDSA).[10,11] Nearly monodisperse cylinders (L_w/L_n < 1.1; L_w and L_n are weight- and number-average lengths, respectively) with controlled lengths from ca. 20 nm to 2 μm

have been obtained using this living CDSA approach by varying the unimer-to-seed ratio.[12] It is also possible to generate complex micelle architectures with segmented coronas including multi-block co-micelles such as monochrome and multi-color fluorescent "barcodes",[10,13,14] multi-armed mi-celles,[15] and non-centrosymmetric structures.[16] The living CDSA process has also been extended to block copolymers containing other crystallizable core-forming blocks, including polylactide,[17] poly(3-hexylthiophene),[18] and polyethylene,[19] as well as to two dimensional structures.[20]

In this Communication we report on our preliminary studies of the block copolymer PFS-ONB-P2VP (ONB = photo-cleavable *o*-nitrobenzyl linker, P2VP = poly(2-vinylpyridine); see structure below). We describe the results of the
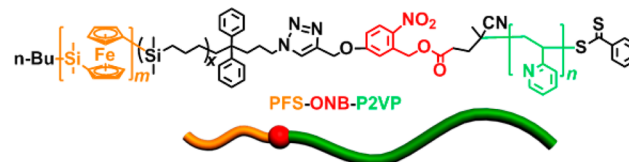
photocleavage chemistry for cylindrical micelles derived from this material and how this leads to an unexpected self-assembly behavior. We also illustrate the synthetic potential of the combination of a photocleavable linker with living CDSA.

The block copolymer PFS_{28}-ONB-$P2VP_{360}$ was synthesized by Cu(I)-catalyzed azide–alkyne cycloaddition of azide-terminated PFS-N_3 and an alkyne-terminated P2VP-ONB material prepared by reversible addition–fragmentation chain transfer (RAFT) polymerization. The method and the characterization of the isolated diblock copolymer PFS_{28}-ONB-$P2VP_{360}$ (M_n = 45.7 kDa and PDI = 1.07) are described in the Supporting Information (Scheme S1, Table S1). The photocleavage of the diblock copolymer (Scheme S1) was monitored by comparing the gel permeation chromatography (GPC) traces of the PFS_{28}-ONB-$P2VP_{360}$ before and after photoirradiation in tetrahydrofuran (THF), a good solvent for both blocks. It was found that the cleavage of the ONB linker was complete within 1 h at a concentration of 1 mg/mL (Figure S4).

Next, cylindrical micelles, M(PFS_{28}-ONB-$P2VP_{360}$), with a very narrow length distribution (1.03 < L_w/L_n < 1.05) (Figure

S6a−c, Table S2), were prepared via the one-dimensional self-seeding living CDSA method.[21] The photocleavage of the $M(PFS_{28}\text{-}ONB\text{-}P2VP_{360})$ cylinders was then performed in isopropanol (iPrOH) containing 2% THF (v/v) at 0.05 mg/mL. The degree of coronal chain cleavage after the photolysis was monitored by GPC (Figure S7). After 0.5 h of irradiation, GPC revealed that ca. 85% of the P2VP corona chains were cleaved from the PFS block, whereas after 2 h this value had increased to greater than ca. 95%.

In our preliminary work described herein, we focused in the materials formed after 1 h of irradiation, in which ca. 90% P2VP corona chains had been cleaved from the PFS block, leaving a nearly bare PFS cylindrical core. Figure 1a shows a transmission
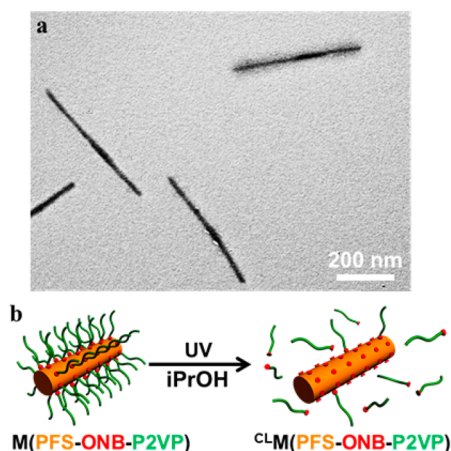

Figure 1. (a) TEM image of a deliberately created mixture of $M(PFS_{28}\text{-}ONB\text{-}P2VP_{360})$ (top right) and photocleaved $^{CL}M(PFS_{28}\text{-}ONB\text{-}P2VP_{360})$ (lower center and left) formed immediately after photoirradiation. (b) Schematic representation of $M(PFS_{28}\text{-}ONB\text{-}P2VP_{360})$ and $^{CL}M(PFS_{28}\text{-}ONB\text{-}P2VP_{360})$.

electron microscopy (TEM) image of a deliberately created mixture of $M(PFS_{28}\text{-}ONB\text{-}P2VP_{360})$ and $^{CL}M(PFS_{28}\text{-}ONB\text{-}P2VP_{360})$ (where ^{CL}M denotes the corona cleaved micelles) to allow comparison on the same carbon film. The P2VP corona, which appeared as a diffuse region of electron density on the periphery of $M(PFS_{28}\text{-}ONB\text{-}P2VP_{360})$ (Figure 1a, top right), was not detected in the case of $^{CL}M(PFS_{28}\text{-}ONB\text{-}P2VP_{360})$ (Figure 1a, lower center and left). Furthermore, atomic force microscopy (AFM) analysis (Figure S9) revealed that both the width and the height of the $^{CL}M(PFS_{28}\text{-}ONB\text{-}P2VP_{360})$ were significantly smaller than those of its precursor. Thus, the height of $^{CL}M(PFS_{28}\text{-}ONB\text{-}P2VP_{360})$ was ca. 11 nm, ca. 60% that of $M(PFS_{28}\text{-}ONB\text{-}P2VP_{360})$ (ca. 18 nm), and the width was reduced to below 60%. The value for the width of $^{CL}M(PFS_{28}\text{-}ONB\text{-}P2VP_{360})$ by TEM was ca. 15 nm, which, based on the height of $^{CL}M(PFS_{28}\text{-}ONB\text{-}P2VP_{360})$ determined by AFM (ca. 11 nm), suggested that the core cross-section was circular or, at most, only slightly elliptical.

Surprisingly, despite removal of the vast majority (up to ca. 95%) of the coronal chains, the $^{CL}M(PFS_{28}\text{-}ONB\text{-}P2VP_{360})$ cylinders do not show a significant tendency to aggregate in solution based on TEM analysis immediately after their preparation by photoirradiation. Thus, only isolated micelles were obtained on solvent evaporation (Figure S10). Interestingly, however, on storage of the colloidal solution of $^{CL}M(PFS_{28}\text{-}ONB\text{-}P2VP_{360})$ with ca. 90% of the corona removed, TEM analysis of dried samples revealed an increasing tendency

for the cylinders to link together via end-to-end coupling over 24 h (Figure S11). In our previous work,[22] we have shown that when dissolved PFS homopolymer is added to cylindrical PFS block copolymer micelles, it functions as a "molecular glue" to connect the cylinders together. It is possible that PFS homopolymer generated in the photocleavage experiment in iPrOH, a poor solvent for PFS, is able, over time, to deposit in small quantities on the cylinder ends and to generate similar elongated superstructures in which cylinders are linked end-to-end (see Figure S12). Lateral aggregation of $^{CL}M(PFS_{28}\text{-}ONB\text{-}P2VP_{360})$ cylinders may be hindered by the residual corona chains as well as the oligomeric carbosilane residues remaining after the photocleavage process.[23]

Next, we explored the ability of the cylinders after coronal cleavage, $^{CL}M(PFS_{28}\text{-}ONB\text{-}P2VP_{360})$, to participate as seed micelles in living CDSA.[10−12] In the case of seeds of $M(PFS_{28}\text{-}ONB\text{-}P2VP_{360})$ cylinders prior to photoirradiation, the expected linear triblock co-micelles (see Figure S13) were formed in iPrOH containing 2% THF (v/v) upon addition of $PFS_{25}\text{-}b\text{-}P2VP_{250}$ unimers. However, in contrast, on addition of $PFS_{25}\text{-}b\text{-}P2VP_{250}$ unimers to $^{CL}M(PFS_{28}\text{-}ONB\text{-}P2VP_{360})$ with ca. 90% of the corona removed (Figure 2a), branched co-micelles with mainly three or four arms (Figures 2c,d and S15) were formed. We have previously demonstrated the formation of branched micelles via the growth of thinner-core cylindrical
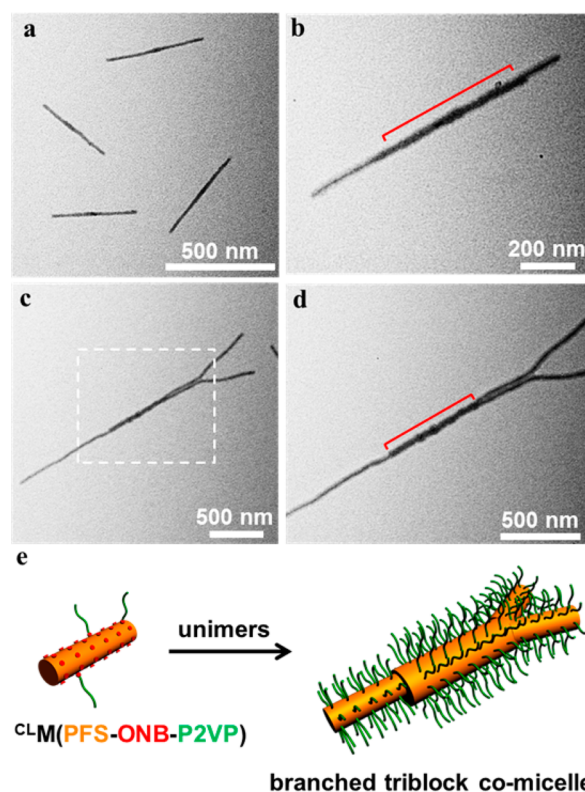

Figure 2. TEM images of (a) $^{CL}M(PFS_{28}\text{-}ONB\text{-}P2VP_{360})$ seeds (prepared immediately after photocleavage); (b) broadened seeds prepared by adding a small amount of $PFS_{25}\text{-}b\text{-}P2VP_{250}$ unimers to the $^{CL}M(PFS_{28}\text{-}ONB\text{-}P2VP_{360})$ seeds (a small amount of growth at the seed ends was also detected); and (c,d) branched triblock comicelles $M(PFS_{25}\text{-}b\text{-}P2VP_{250})\text{-}b\text{-}^{CL}M(PFS_{28}\text{-}ONB\text{-}P2VP_{360})\text{-}b\text{-}M(PFS_{25}\text{-}b\text{-}P2VP_{250})$ prepared by adding a large amount of unimers to the $^{CL}M(PFS_{28}\text{-}ONB\text{-}P2VP_{360})$ seeds. The red brackets mark the broadened seeds. (e) Scheme depicting the CDSA process.

micelles at the termini of the thicker-core cylindrical micelle seeds.[24] In such cases, the length of the PFS core-forming block for the added unimers was substantially less than that in the seeds. However, in the current case, both the added unimers (PFS$_{25}$-b-P2VP$_{250}$) and the seed cylinder ^{CL}M(PFS$_{28}$-ONB-P2VP$_{360}$) possessed very similar PFS block lengths. This provided evidence that corona removal has an important influence on the cylinder behavior with respect to living CDSA.

Our initial postulate to explain the different behavior was that corona removal at the cylinder termini leaves the exposed core more accessible to incoming unimers and more than one cylinder is then able to grow from the PFS surface. In order to obtain further insight into the branched micelle formation, the addition of a small quantity of PFS$_{25}$-b-P2VP$_{250}$ unimers to the ^{CL}M(PFS$_{28}$-ONB-P2VP$_{360}$) seeds was monitored by TEM. This showed that, in the early stages of the process, the seeds became broader (Figure 2b, marked with red bracket), and this precedes substantial elongation via unimer addition at the termini (Figure 2c,d). The thickening apparently occurred relatively uniformly along the entire ^{CL}M(PFS$_{28}$-ONB-P2VP$_{360}$) seed. Analysis by TEM (Figure 2b) indicated that the width of the PFS core of the "broadened seeds" was ca. 21 nm, compared to ca. 15 nm for the original ^{CL}M(PFS$_{28}$-ONB-P2VP$_{360}$) seeds in Figure 2a. AFM analysis (Figure S14) also confirmed that the height of the broadened seeds was much larger (ca. 23 nm versus ca. 11 nm). These observations indicate that removal of the corona chains allows the addition of block copolymer unimers to the side of cylinder. This type of growth at the sides of cylinders rather than at the termini is very rare but not unprecedented in CDSA experiments. Examples have been previously noted when unimers with large PFS volume fractions or PFS homopolymers were added to cylindrical seeds with their full complement of coronal chains.[22]

In order to further explore the synthetic potential of the combination of a photocleavable linker with living CDSA, we investigated the preparation of uniform P2VP nanotubes. Although many examples of nanotubes have previously been prepared from block copolymers,[9c,25] the use of living CDSA offers the possibility of length control and the formation of monodisperse samples. Our adopted strategy involved the use of well-defined M(PFS$_{28}$-ONB-P2VP$_{360}$) cylinders as precursors together with corona cross-linking,[26] an important method for the creation of stabilized block copolymer assemblies. Nanotubes were prepared via a one-step, parallel corona cross-linking/ONB junction cleavage process after the pendent pyridyl groups in the corona of the cylinders (L_n = 900 nm, L_w/L_n = 1.02) had been quaternized with 4-vinylbenzyl chloride in iPrOH to form ^{Q}M(PFS$_{28}$-ONB-P2VP$_{360}$) (Figure 3a,b). The corona of the cylinder appeared slightly darker by TEM after the quaternization, consistent with an increase in electron density (Figure S16a).

After 1 h of photoirradiation of ^{Q}M(PFS$_{28}$-ONB-P2VP$_{360}$) in the presence of dimethoxy-2-phenylacetophenone (dmpap) as photoinitiator to cross-link the 4-vinylbenzyl units and to cleave the ONB linker (in iPrOH containing 10% DMSO to prevent micelle aggregation), much thicker structures were observed by TEM (width ca. 28 nm, see Figure S16b). This, together with the retention of micelle integrity in 70% THF, a medium in which PFS and ^{Q}P2VP/P2VP are soluble (Figure S16d), indicated that corona cross-linking had been achieved. During the photoirradiation process, the photoreleased PFS core appeared to aggregate into small particles, which were observed as regions of high electron density (Figure S16b, inset).
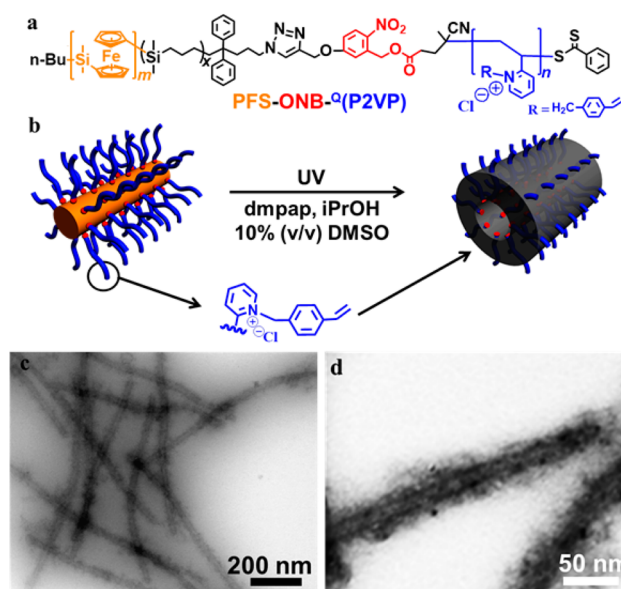

Figure 3. (a) Structure of the quaternized diblock copolymer. (b) Schematic representation of ^{Q}M(PFS$_{28}$-ONB-P2VP$_{360}$) and nanotube formation. (c,d) TEM images of ^{Q}M(PFS$_{28}$-ONB-P2VP$_{360}$) after photolysis in iPrOH and DMSO (10% v/v) for 1 h. The sample was stained by RuCl$_3$.

To provide further characterization of the nanotubes, the pyridyl groups were stained with RuCl$_3$ followed by TEM analysis (Figures 3c,d and S17a−c). TEM revealed that the average width of the inner cavity was ca. 13 nm, which is consistent with the diameter of the PFS core in ^{Q}M(PFS$_{28}$-ONB-P2VP$_{360}$) (ca. 13 nm, Figure S18). Comparative compositional analysis of the nanotubes and the M(PFS$_{28}$-ONB-P2VP$_{360}$) precursor was achieved by spot energy-dispersive X-ray analysis. This provided convincing evidence that the PFS core had been removed in the nanotubes, as no peak for Fe was detected (see Figure S19). Consistent with removal of the crystalline core, AFM revealed a slightly collapsed nanostructure of reduced height (12 nm vs 18 nm, Figure S21).

To explore the versatility and control inherent in the synthetic strategy, we attempted to prepare uniform nanotubes of different lengths. We used two samples of nearly monodisperse M(PFS$_{28}$-ONB-P2VP$_{360}$) cylinder precursors (L_n = 490 and 180 nm, L_w/L_n ≤ 1.05). By TEM the resulting nanotubes (Figures 4 and S20) were of the same length and length polydispersity within experimental error (Table S3).[12] The outer diameter of the nanotube was ca. 28 nm and, based
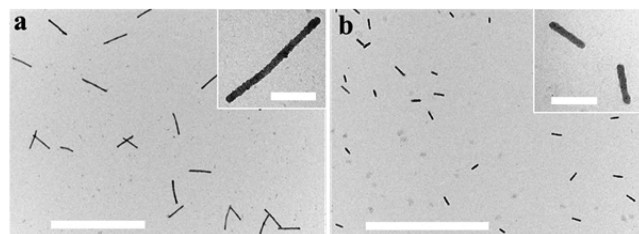

Figure 4. TEM images of ^{Q}M(PFS$_{28}$-ONB-P2VP$_{360}$) after photolysis in iPrOH containing 10% DMSO (v/v) for 1 h. The contour lengths of the resulting nanotubes are (a) 490 nm, L_w/L_n = 1.05, and (b) 180 nm, L_w/L_n = 1.04. Scale bars are 2 μm and, for the inset, 200 nm.

on an inner cavity of 13 nm, the outer shell thickness was ca. 7.5 nm.

In summary, our preliminary studies of the PFS-ONB-P2VP diblock copolymer have revealed that photocleavage leads to cylinders that are surprisingly colloidally stable, permitting their use in living CDSA processes to create branched micelles. A combination of the ability to form PFS-ONB-P2VP cylinders by living CDSA, the presence of a photocleavable block junction, and corona cross-linking allowed the preparation of nearly monodisperse samples of cross-linked P2VP nanotubes of controlled length. Future work will involve in-depth studies of cylinders with different degrees of coronal cleavage and a further exploration of the synthetic possibilities for the creation of new self-assembled nanomaterials, such as segmented multi-armed nanotubes.

■ ASSOCIATED CONTENT

Ⓢ Supporting Information

Experimental procedures and additional data. This material is available free of charge via the Internet at http://pubs.acs.org.

■ AUTHOR INFORMATION

Corresponding Authors

*mwinnik@chem.utoronto.ca
*ian.manners@bristol.ac.uk

Notes

The authors declare no competing financial interest.

■ ACKNOWLEDGMENTS

■ REFERENCES

(1) (a) Mai, Y. Y.; Eisenberg, A. *Chem. Soc. Rev.* **2012**, *41*, 5969–5985. (b) Moughton, A. O.; Hillmyer, M. A.; Lodge, T. P. *Macromolecules* **2012**, *45*, 2–19. (c) Schacher, F. H.; Rupar, P. A.; Manners, I. *Angew. Chem., Int. Ed.* **2012**, *51*, 7898–7921.

(2) (a) Cui, H.; Chen, Z.; Zhong, S.; Wooley, K. L.; Pochan, D. J. *Science* **2007**, *317*, 647–650. (b) Groeschel, A. H.; Schacher, F. H.; Schmalz, H.; Borisov, O. V.; Zhulina, E. B.; Walther, A.; Mueller, A. H. E. *Nat. Commun.* **2012**, *3*, 710. (c) Groeschel, A. H.; Walther, A.; Loebling, T. I.; Schacher, F. H.; Schmalz, H.; Mueller, A. H. E. *Nature* **2013**, *503*, 247–251.

(3) (a) Dupont, J.; Liu, G.; Niihara, K.; Kimoto, R.; Jinnai, H. *Angew. Chem., Int. Ed.* **2009**, *48*, 6144–6147. (b) Zhong, S.; Cui, H.; Chen, Z.; Wooley, K. L.; Pochan, D. J. *Soft Matter* **2008**, *4*, 90–93.

(4) (a) Huang, H.; Chung, B.; Jung, J.; Park, H.-W.; Chang, T. *Angew. Chem., Int. Ed.* **2009**, *48*, 4594–4597. (b) Li, X.; Gao, Y.; Xing, X.; Liu, G. *Macromolecules* **2013**, *46*, 7436–7442. (c) Pochan, D. J.; Chen, Z. Y.; Cui, H. G.; Hales, K.; Qi, K.; Wooley, K. L. *Science* **2004**, *306*, 94–97.

(5) Gil, E. S.; Hudson, S. M. *Prog. Polym. Sci.* **2004**, *29*, 1173–1222.

(6) (a) Rodríguez-Hernández, J.; Chécot, F.; Gnanou, Y.; Lecommandoux, S. *Prog. Polym. Sci.* **2005**, *30*, 691–724. (b) Rijcken, C. J. F.; Soga, O.; Hennink, W. E.; van Nostrum, C. F. *J. Controlled Release* **2007**, *120*, 131–148. (c) Zhao, Y. *Macromolecules* **2012**, *45*, 3647–3657.

(7) (a) Huang, Y.; Dong, R.; Zhu, X.; Yan, D. *Soft Matter* **2014**, *10*, 6121–6138. (b) Zhao, Y. *J. Mater. Chem.* **2009**, *19*, 4887–4895. (c) Schumers, J.-M.; Fustin, C.-A.; Gohy, J.-F. *Macromol. Rapid Commun.* **2010**, *31*, 1588–1607.

(8) (a) Wang, G.; Tong, X.; Zhao, Y. *Macromolecules* **2004**, *37*, 8911–8917. (b) Jiang, J. Q.; Tong, X.; Zhao, Y. *J. Am. Chem. Soc.* **2005**, *127*, 8290–8291. (c) Menon, S.; Ongungal, R. M.; Das, S. *Polym. Chem.* **2013**, *4*, 623–628. (d) Rabnawaz, M.; Liu, G. *Macromolecules* **2012**, *45*, 5586–5595. (e) Rabnawaz, M.; Liu, G. *Macromolecules* **2014**, *47*, 5115–5123. (f) Yan, B.; Boyer, J.-C.; Branda, N. R.; Zhao, Y. *J. Am. Chem. Soc.* **2011**, *133*, 19714–19717. (g) Bertrand, O.; Schumers, J.-M.; Kuppan, C.; Marchand-Brynaert, J.; Fustin, C.-A.; Gohy, J.-F. *Soft Matter* **2011**, *7*, 6891–6896.

(9) (a) Cabane, E.; Malinova, V.; Meier, W. *Macromol. Chem. Phys.* **2010**, *211*, 1847–1856. (b) Xuan, J.; Han, D.; Xia, H.; Zhao, Y. *Langmuir* **2014**, *30*, 410–417. (c) Yan, Q.; Xin, Y.; Zhou, R.; Yin, Y.; Yuan, J. *Chem. Commun.* **2011**, *47*, 9594–9596. (d) Nazemi, A.; Gillies, E. R. *Chem. Commun.* **2014**, *50*, 11122–11125. (e) Yang, H.; Jia, L.; Wang, Z.; Di-Cicco, A.; Lévy, D.; Keller, P. *Macromolecules* **2011**, *44*, 159–165.

(10) Gaedt, T.; Ieong, N. S.; Cambridge, G.; Winnik, M. A.; Manners, I. *Nat. Mater.* **2009**, *8*, 144–150.

(11) Wang, X.; Guerin, G.; Wang, H.; Wang, Y.; Manners, I.; Winnik, M. A. *Science* **2007**, *317*, 644–647.

(12) Gilroy, J. B.; Gaedt, T.; Whittell, G. R.; Chabanne, L.; Mitchels, J. M.; Richardson, R. M.; Winnik, M. A.; Manners, I. *Nat. Chem.* **2010**, *2*, 566–570.

(13) He, F.; Gaedt, T.; Manners, I.; Winnik, M. A. *J. Am. Chem. Soc.* **2011**, *133*, 9095–9103.

(14) Hudson, Z. M.; Lunn, D. J.; Winnik, M. A.; Manners, I. *Nat. Commun.* **2014**, *5*, 3372.

(15) Qiu, H.; Cambridge, G.; Winnik, M. A.; Manners, I. *J. Am. Chem. Soc.* **2013**, *135*, 12180–12183.

(16) Rupar, P. A.; Chabanne, L.; Winnik, M. A.; Manners, I. *Science* **2012**, *337*, 559–562.

(17) (a) Pitto-Barry, A.; Kirby, N.; Dove, A. P.; O'Reilly, R. K. *Polym. Chem.* **2014**, *5*, 1427–1436. (b) Petzetakis, N.; Dove, A. P.; O'Reilly, R. K. *Chem. Sci.* **2011**, *2*, 955–960.

(18) (a) Patra, S. K.; Ahmed, R.; Whittell, G. R.; Lunn, D. J.; Dunphy, E. L.; Winnik, M. A.; Manners, I. *J. Am. Chem. Soc.* **2011**, *133*, 8842–8845. (b) Qian, J.; Li, X.; Lunn, D. J.; Gwyther, J.; Hudson, Z. M.; Kynaston, E.; Rupar, P. A.; Winnik, M. A.; Manners, I. *J. Am. Chem. Soc.* **2014**, *136*, 4121–4124. For related work, see: (c) Kamps, A. C.; Fryd, M.; Park, S.-J. *ACS Nano* **2012**, *6*, 2844–2852. (d) Lee, I.-H.; Amaladass, P.; Yoon, K.-Y.; Shin, S.; Kim, Y.-J.; Kim, I.; Lee, E.; Choi, T.-L. *J. Am. Chem. Soc.* **2013**, *135*, 17695–17698.

(19) Schmelz, J.; Schedl, A. E.; Steinlein, C.; Manners, I.; Schmalz, H. *J. Am. Chem. Soc.* **2012**, *134*, 14217–14225.

(20) Hudson, Z. M.; Boott, C. E.; Robinson, M. E.; Rupar, P. A.; Winnik, M. A.; Manners, I. *Nat. Chem.* **2014**, *6*, 893–898.

(21) Qian, J.; Guerin, G.; Lu, Y.; Cambridge, G.; Manners, I.; Winnik, M. A. *Angew. Chem., Int. Ed.* **2011**, *50*, 1622–1625.

(22) Yusoff, S. F. M.; Gilroy, J. B.; Cambridge, G.; Winnik, M. A.; Manners, I. *J. Am. Chem. Soc.* **2011**, *133*, 11220–11230.

(23) Cleavage of the ONB group should leave oligo(dimethylsila-cyclobutane)s with a terminal triazole-linked aromatic residue attached to the PFS chains in the core (see Scheme S1).

(24) Qiu, H.; Du, V. A.; Winnik, M. A.; Manners, I. *J. Am. Chem. Soc.* **2013**, *135*, 17739–17742.

(25) (a) Liu, G. In *Self-Assembled Nanomaterials II: Nanotubes*; Shimizu, T., Ed.; Springer: Berlin, 2008; Vol. 220, pp 29–64. (b) Cheng, C.; Qi, K.; Khoshdel, E.; Wooley, K. L. *J. Am. Chem. Soc.* **2006**, *128*, 6808–6809. (c) Grumelard, J.; Taubert, A.; Meier, W. *Chem. Commun.* **2004**, 1462–1463. (d) Yan, X. H.; Liu, G. J.; Li, Z. *J. Am. Chem. Soc.* **2004**, *126*, 10059–10066. For related work, see: (e) Wang, Y.; Huang, Z.; Kim, Y.; He, Y.; Lee, M. *J. Am. Chem. Soc.* **2014**, *136*, 16152–16155.

(26) (a) Thurmond, K. B.; Kowalewski, T.; Wooley, K. L. *J. Am. Chem. Soc.* **1996**, *118*, 7239–7240. (b) O'Reilly, R. K.; Hawker, C. J.; Wooley, K. L. *Chem. Soc. Rev.* **2006**, *35*, 1068–1083. (c) Ding, J.; Liu, G. *Macromolecules* **1998**, *31*, 6554–6558.